

Hydrogenation of the Nanopowders That Form in a Carbon–Helium Plasma Stream during the Introduction of Ni and Mg

G. N. Churilov^{a,*}, I. V. Osipova^a, Ye. V. Tomashevich^b, G. A. Glushchenko^a, A. S. Fedorov^a,
Z. I. Popov^a, N. V. Bulina^c, S. N. Vereshchagin^b, A. M. Zhizhaev^b, and A. V. Cherepakhin^a

^aKirensky Institute of Physics, Siberian Branch, Russian Academy of Sciences, Krasnoyarsk, 660036 Russia

*e-mail: churilov@iph.krasn.ru

^bInstitute of Chemistry and Chemical Technology, Siberian Branch, Russian Academy of Sciences,
ul. K. Marksa 42, Krasnoyarsk, 660049 Russia

^cInstitute of Solid State Chemistry and Mechanochemistry, Siberian Branch, Russian Academy of Sciences,
ul. Kutateladze 18, Novosibirsk, 630128 Russia

Received August 12, 2010; in final form, April 21, 2011

Abstract—Composite nanoparticles consisting of magnesium, nickel, and carbon atoms are studied both theoretically and experimentally. The calculations performed in terms of the density functional theory show that the jump frequency of hydrogen atoms in nickel-containing magnesium hydride increases substantially near impurity nickel atoms; as a result, the rate of hydrogen absorption by magnesium also increases. Nickel on the magnesium surface is shown to be absorbed via an island growth mechanism. Composite Mg–C, Ni–C, and Mg–Ni–C powders are produced by plasmachemical synthesis in a carbon–helium plasma stream. Hydrogen is introduced into a chamber during synthesis. It is found by X-ray photoelectron spectroscopy and thermogravimetric analysis that, among these three composites, only Mg–Ni–C contains magnesium fixed in the MgH₂ compound. The process of such “ultrarapid” hydrogenation of magnesium, which occurs in the time of formation of composite nanoparticles, can be explained by the catalytic action of nickel, which is enhanced by a high temperature. Scanning electron microscopy micrographs demonstrate the dynamics of the dehydrogenation of Mg–Ni–C composite nanoparticles in heating by an electron beam.

DOI: 10.1134/S1063776111140135

1. INTRODUCTION

The consumption of hydrocarbon fuel is increasing substantially, which leads to an increase in its cost and the number of ecological problems. As a result, interest in alternative energy sources has quickened. Hydrogen power engineering is one of the promising trends in solving ecological problems. The use of electrical engines instead of internal combustion engines will make it possible to solve most problems related to transport. One of the two aspects of hydrogen power engineering, namely, the conversion of the chemical energy that is liberated during the oxidation of hydrogen by oxygen into electric power has been solved due to the development of hydrogen fuel cells. The other aspect, namely, storage and transportation of hydrogen with a high specific density is at the initial stage of its solution. The storage and transportation of hydrogen in cryogenic and high-pressure cylinders cannot solve this problem mainly because of the large mass of the auxiliary equipment, which eventually leads to a low density of stored hydrogen, and because of the impossibility of providing safe conditions of their operation. Therefore, great efforts are made to find effective sorbents to accumulate hydrogen to a generally accepted level of 6.5 wt %.

Many research groups are searching for the possibilities of creating effective hydrogen storage cells based on new composites of hydride-forming metals, including metal nanoclusters. Magnesium is a promising metal for hydrogen adsorption due to its low molar weight, low cost, availability, and the absence of toxicity. Magnesium is known to form hydride MgH₂, in which the hydrogen content of is 7.6 wt % [1]. One of the significant problems that hinder the use of magnesium is low absorption and desorption rates. Experimental data demonstrate that one of the causes of a low hydrogen absorption rate in magnesium is a low hydrogen diffusion rate in its crystal lattice even at a relatively high temperature (300–400°C). The hydrogen absorption in the crystal structure is retarded by lattice dilatation, which results in defect accumulation and cracking. These problems can be solved by the use of nanoparticles instead of a bulk material. In this case, the hydrogen saturation rate increases due to an increase in the surface-to-volume ratio, and cracking is absent. Another cause of slow hydrogen absorption by magnesium is related to difficult dissociation of hydrogen molecules on the magnesium surface before hydrogen diffusion into its volume. Many *d* metals, e.g., nickel and palladium, have good catalytic properties to improve the dissociation of H₂ molecules. The

presence of such a metal in magnesium particles, especially in their surface layers, should substantially accelerate this dissociation.

Therefore, composite nanoparticles containing Mg and Ni, i.e., a catalytic metal and a hydride-forming metal, are promising materials for hydrogen storage. In this case, the catalyst can accelerate sorption and desorption processes by several thousands times.

Nowdays, the main method used to produce nanocomposites is mechanical alloying (MA), which is effective to produce materials of various compositions and microstructures (including thermodynamically immiscible components). This method is successfully used to make various substances to be applied as hydrogen storage cells [2, 3]. The MA method represents the “top down” approach, in which nanoparticles are formed by milling of macroscopic particles into nanoparticles.

In this work, we study composite magnesium-containing nanoparticles produced in the carbon–helium plasma of a high-frequency arc discharge. This method differs from MA in the fact that synthesis occurs at high temperatures (~ 5000 K) and nanoparticles form according to the “bottom up” approach, i.e., from individual atoms. In this approach, particles usually have a more uniform distribution of their elements, which is the main prerequisite of increasing the rate of hydrogen absorption by such particles.

2. THEORETICAL RESULTS

We performed ab initio calculations using the VASP (Vienna Ab initio Simulation Package) software package [4] to study the effect of nickel on the diffusion rate of hydrogen atoms inside magnesium hydride. VASP uses a pseudopotential and the expansion of wavefunctions in a plane wave basis in terms of the density functional theory (DFT) [5]. For an exchange–correlation potential, we used the generalized gradient approximation (GGA) and the Perdew–Burke–Ernzerhof (PBE) functional. To effectively decrease the number of basis functions, we used the Vanderbilt ultrasoft potentials, which make it possible to significantly decrease cutoff energy E_{cutoff} (which determines the maximum kinetic energy) and, correspondingly, the calculation time. The geometry of all systems was optimized until the forces on all atoms were weaker than 0.05 eV/Å. The integration inside the irreducible part of the first Brillouin zone was performed only at point Γ because of large supercell sizes.

We simulated the introduction of a small number of nickel atoms into magnesium. The computation details were similar to those in our previous work [6]. The binding energy of a nickel atom in the magnesium lattice ($E_{\text{Ni–Mg}} = 1.27$ eV) was calculated for an insulated nickel atom in a supercell consisting of

53 magnesium atoms. Binding energy $E_{\text{Ni–Mg}}$ was calculated as

$$E_{\text{Ni–Mg}} = E_{\text{Mg53Ni}} - 53E_{\text{Mg}} - E_{\text{Ni}}, \quad (1)$$

where the binding energy per magnesium atom E_{Mg} was calculated from the binding energy of the crystal, as in the case of nickel. A positive binding energy of nickel means that nickel atoms can be incorporated into the magnesium lattice only at a low concentration, since the contribution of the configurational entropy

$$-TS = T \ln \left(\frac{\theta}{1-\theta} \right)$$

(where θ is the Ni atom concentration in the Mg matrix) to the Gibbs free energy $G = E_{\text{bind}} + P\Omega - TS$ becomes substantial and leads to the penetration of Ni atoms into the Mg lattice.

We also studied the effect of nickel atoms on the migration of hydrogen atoms in the MgH_2 lattice with vacancies. Hydrogen atom jump frequencies k were calculated using the theory of a transient state and the following well-known Vineyard formula, which generalizes an Arrhenius-type formula [7]:

$$k = A \exp(-E_{\text{bar}}/kT), \quad (2)$$

where T is the temperature and E_{bar} is the potential barrier to a hydrogen atom jump between the two nearest potential minima. We calculated E_{bar} with the nudged elastic band method [8]. Preexponential factor A was determined as

$$A = \frac{kT}{h} \prod_{i=1}^{3N-4} \left(1 - \exp\left(-\frac{h\nu_i}{kT}\right) \right) \times \left[\prod_{i=1}^{3N-3} \left(1 - \exp\left(-\frac{h\nu_i}{kT}\right) \right) \right]^{-1}. \quad (3)$$

The product

$$\prod_{i=1}^{3N-3} \left(1 - \exp\left(-\frac{h\nu_i}{kT}\right) \right),$$

which includes all phonon oscillation frequencies ν_i of the system, except oscillations corresponding to uniform translations of the lattice was calculated for the local minima of hydrogen atom sites, and the product

$$\prod_{i=1}^{3N-4} \left(1 - \exp\left(-\frac{h\nu_i}{kT}\right) \right)$$

was calculated for hydrogen atom vibrations at the saddle point of the hydrogen motion trajectory between two minima. The potential barrier to a hydrogen atom jump in MgH_2 was calculated to be $E_{\text{bar}} = 1.05$ eV. After the substitution of a nickel atom for a magnesium atom, the potential barrier to a hydrogen jump near the nickel atom changes. The potential barriers to an H atom jump between the minima in the second coordination shell of a Ni atom (0.90 eV) and,

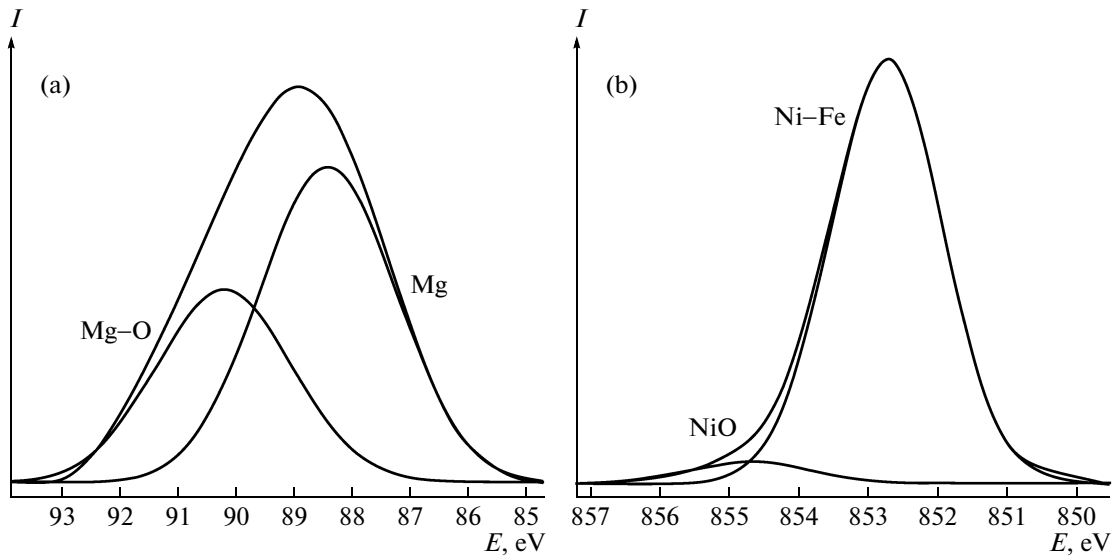


Fig. 1. XPS spectra: (a) magnesium line in an Mg–C composite and (b) nickel line in an Ni–C composite.

especially, in the first coordination shell (0.40 eV) are significantly lower than those for the case of pure magnesium hydride MgH_2 . The binding energy of a hydrogen atom in the first coordination shell of nickel is approximately 1 eV lower than for the second coordination shell. This means that hydrogen atoms should concentrate in the nearest vicinity of nickel atoms, and the hydrogen jump frequency near nickel atoms should increase significantly. Using Eq. (2), we can easily find that the hydrogen jump frequency near nickel atoms at $T = 300$ K should increase by a factor of 350.

We also simulated the structure of an Ni coating on the Mg(0001) surface. We calculated the binding energy of a cluster consisting of one and two 16-atom nickel layers on the Mg surface, which was taken to be a periodic and infinite plate (slab geometry). To calculate binding energy of nickel E_{Ni} in these layers, we used formulas similar to Eq. (1). The values of E_{Ni} calculated for one and two Ni atomic layers are 1.42 and 1.25 eV/atom, respectively. As follows from a comparison of these values with the binding energy calculated for a bulk nickel crystal E_{Ni} (which corresponds to coating of an infinite thickness and is -5.10 eV/atom), nickel on the magnesium surface should form multi-layer clusters according to an island growth mechanism rather than a single-layer epitaxial coating. As the nickel coating thickness on the surface increases, the binding energy of nickel E_{Ni} tends toward the value of E_{Ni} characteristic of a bulk crystal.

3. EXPERIMENTAL RESULTS

Composite Mg–C, Ni–C, and Mg–Ni–C nanoparticles were synthesized in a helium flow, in a high-frequency arc plasma. The arc glowed in the gap

between a graphite bush and a graphite rod [9]. Magnesium and nickel powders were introduced with a helium flow (4 l/min) during synthesis, and hydrogen was also let in a chamber (0.4 l/min). The iron content in the sputtered graphite electrodes was 0.3 at %, and the iron content in all synthesized samples was 2–2.5 at %.

The samples were examined by X-ray photoelectron spectroscopy (XPS) on an ultrahigh-vacuum SPECS photoelectron spectrometer using AlK_α radiation and by scanning electron microscopy (SEM) on a high-resolution Hitachi S-5500 electron microscope. Thermogravimetric (TG) analysis was performed with a synchronous NETZSCH STA 449C-QMS analyzer in the temperature range 40–1000°C at a heating rate of 10°C/min, an Ar flow rate of 40 ml/min, and an oxygen content of 0.01 vol % in the flow.

The XPS data demonstrate that the composition of the carbon condensate formed upon the introduction of Mg and H_2 in a helium flow is as follows: 68 at % C, 20.9 at % O, 9 at % Mg, and 2.1 at % Fe. Using the binding energy distribution of the 1s line of C, we identified the hybridization of pure carbon as sp^2 and sp^3 (64 and 24% of the area under the 1s line, respectively) and detected C–O and C=O bonds (6 and 4% of the area under the 1s line, respectively). An insignificant amount of carbon is fixed by Mg. The binding energies of the 2s line of Mg correspond to the free state of Mg and the Mg–O chemical bond (62 and 38% of the area under the 2s line, respectively; see Fig. 1a).

We also performed a synthesis in which Ni and H_2 were introduced into a carbon–helium plasma stream. With XPS, the composition of the carbon condensate was found to be 75.7 at % C, 10.5 at % O, 11.3 at % Ni, and 2.5 at % Fe. The binding energy distribution of the

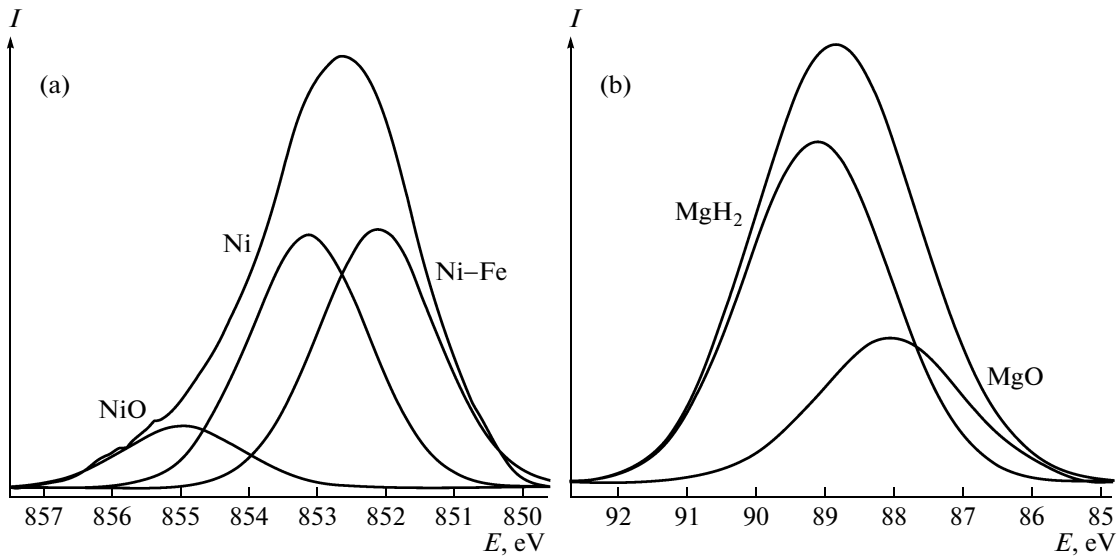


Fig. 2. XPS spectra of an Mg–Ni–C composite: (a) nickel line and (b) magnesium line.

2*p* line of Ni indicates that the major part of nickel (95% of the area under the 2*p* line) is fixed by iron and the other part forms oxide (5% of the area under the 2*p* line; see Fig. 1b). The catalytic effect of nickel manifests itself in increasing the component corresponding to the *sp*² hybridization of carbon (77% of the area under the 1*s* line of C) in the binding energy distribution of the 1*s* line of C and decreasing the component corresponding to the *sp*³ hybridization of carbon (16% of the area under the 1*s* line of C). The other carbon is also fixed by oxygen. These facts indicate that nickel nanoparticles favor the formation of planar carbon forms.

We then performed a synthesis in which Mg, Ni, and H₂ were simultaneously introduced into a car-

bon–helium plasma stream. With XPS, the composition of the carbon condensate was found to be 71.6 at % C, 19.1 at % O, 0.8 at % Ni, 2.1 at % Fe, and 6.4 at % Mg. The binding energy distribution of the 2*p* line of Ni (Fig. 2a) indicates that Ni in the carbon condensate is both in a free state and in a compound with Fe and O (45, 44, and 11% of the area under the 2*p* line of Ni, respectively). Most part of Mg forms hydride MgH₂ (70% of the area under the 2*s* line of Mg), and the remaining part of magnesium forms oxide MgO (30% of the area under the 2*s* line of Mg; see Fig. 2b). The presence of a high magnesium content in the hydride state and the absence of magnesium in the sample fabricated without nickel suggest a significant catalytic action of nickel on the hydrogen absorption by magnesium nanoparticles. A possible effect of iron should be excluded, since the same iron content was detected in the synthesized composite magnesium–carbon nanoparticles and no hydrogen absorption with the formation of MgH₂ was observed.

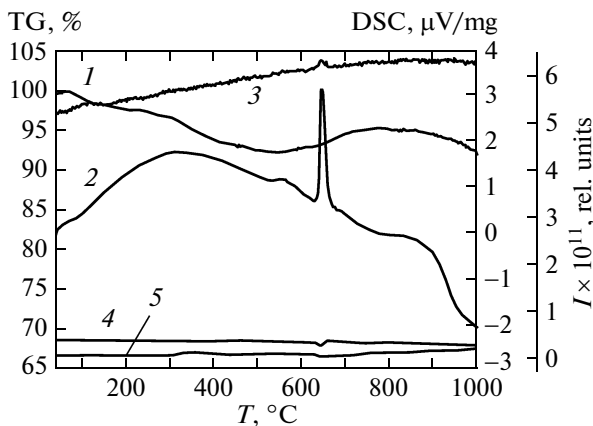


Fig. 3. Oxidation thermogram of an Mg–Ni–C composite: (1) weight change; (2) heat release; and (3–5) intensity curves for H₂O ($m/z = 18$), O₂ (32), and CO₂ (44), respectively.

Figure 3 shows the results of TG analysis of the carbon condensate fabricated by the introduction of Ni and Mg. The sample weight loss at the initial stage of heating corresponds to the loss of adsorbed water (1.4 wt %). The sample weight loss in the temperature range 120–640°C is related to the burn-out of amorphous carbon, nanotubes, and hydrogen adsorbed by these products. This finding is supported by the heat-release curves and the ion current curves for the CO₂ and H₂O masses (Fig. 3; curves 2, 5, 3). The heat released at a temperature of 644.3°C is accompanied by water liberation and noticeable absorption of oxygen from the gas phase (Fig. 3; curves 2, 3, 4). This process lasts for 4 min and is obviously related to the oxidation and transformation of MgH₂ into MgO (Fig. 3). The further sample weight loss is associated

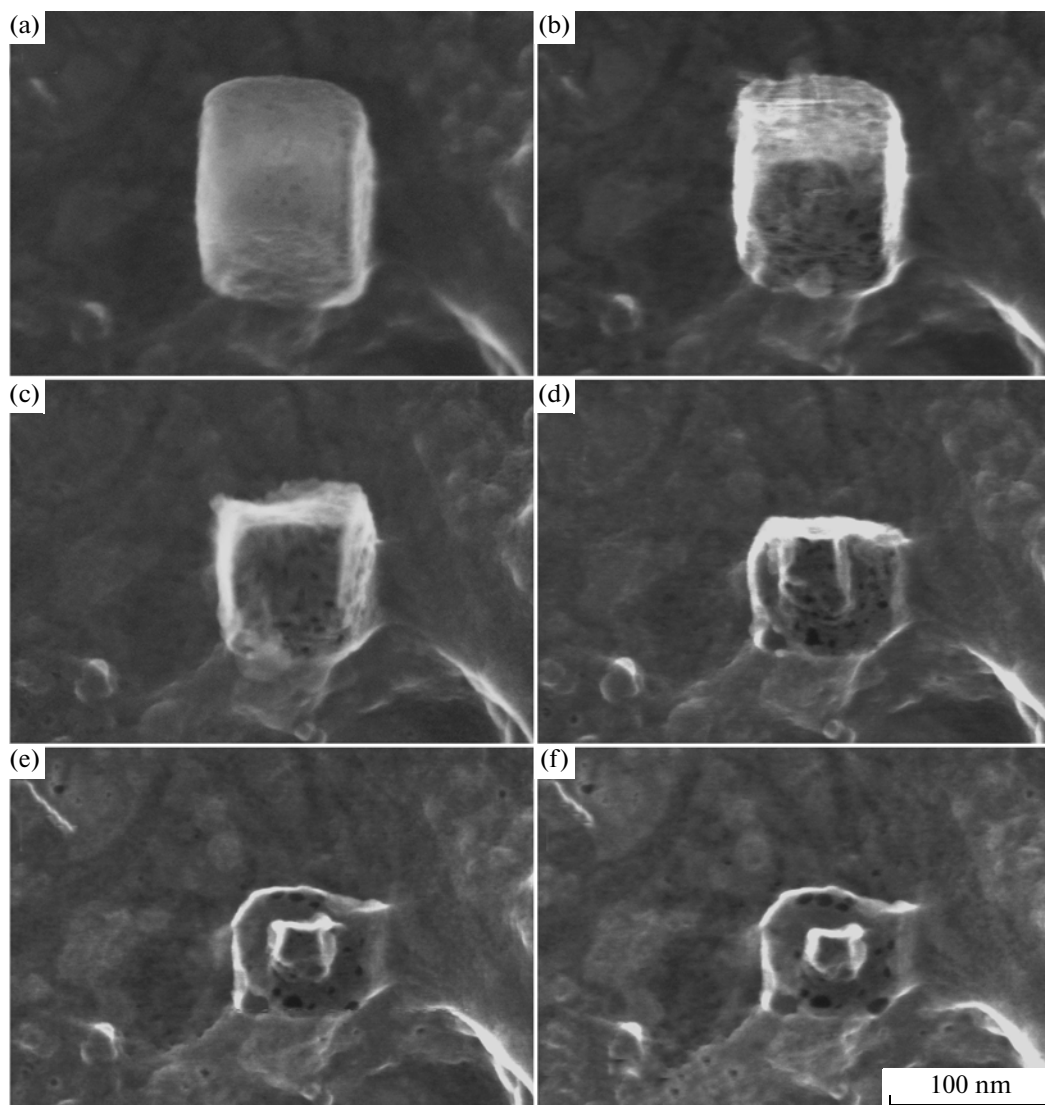


Fig. 4. SEM images of an Mg–Ni–C composite particle at various electron beam action times at 30 kV: (a) 0, (b) 60, (c) 120, (d) 180, (e) 300, and (f) 480 s.

with the burn-out of the remaining graphite, and the additionally released energy is attributed to restructuring in metal nanoparticles. These processes correspond to the temperature dependence of the sample weight (Fig. 3, curve *I*).

With SEM, we were able to observe the dynamics of the dehydrogenation process described above. Under an electron beam, many particles rapidly changed their shape, decreased in size, and then stabilized. Figure 4 shows a series of sequential micrographs of an Mg–Ni–C composite particle to demonstrate the dehydrogenation process.

4. CONCLUSIONS

With DFT calculations, we determined the jump frequency of hydrogen atoms in magnesium hydride

near nickel atoms, which was found to be higher than that in pure hydride MgH_2 by a factor of 350 (at $T = 300$ K). The calculated binding energies of nickel on the magnesium surface correspond to its condensation according to an island growth mechanism. Our experimental results demonstrate that Mg–C and Ni–C composites do not form hydrides during a plasma-chemical synthesis in which H_2 was introduced into a helium flow. The hydrogenation of Mg during a plasma-chemical synthesis in which H_2 was introduced into a helium flow takes place in an Mg–Ni–C composite in a short time, which corresponds to its formation. Most part of magnesium ($\sim 70\%$) in the Mg–Ni–C composite forms hydride MgH_2 . Dehydrogenation occurs at a temperature of 644.3°C within 4 min.

Thus, our theoretical and experimental results demonstrate that the presence of Ni in an Mg–Ni–C

composite substantially accelerates hydrogenation, so that the time of formation of composite nanoparticles in a hydrogen-containing plasma is sufficient for magnesium hydrogenation.

ACKNOWLEDGMENTS

We thank the Interdisciplinary Supercomputer Center of the Russian Academy of Sciences (Moscow) and the Computer Simulation Institute, Siberian Branch, Russian Academy of Sciences (Krasnoyarsk) for providing the computation abilities of their supercomputers, which were used to perform all quantum-mechanical calculations.

This work was supported by the Russian Foundation for Basic Research, project no. 09-03-00383-a.

REFERENCES

1. H. Buchner, P. Pelloux-Gervais, M. Müller, F. Grafwallner, and P. Luger, in *Hydrogen and Other Alternative Fuels for Air and Ground Transportation*, Ed. by H. W. Pohl (Wiley, Chichester, United Kingdom, 1995), p. 7.
2. A. Zaluska, L. Zaluski, and J. O. Ström-Olsen, *Appl. Phys. A: Mater. Sci. Process.* **72**, 157 (2001).
3. J. Huot, G. Liang, and R. Schulz, *Appl. Phys. A: Mater. Sci. Process.* **72**, 187 (2001).
4. G. Kresse and J. Furthmüller, *Phys. Rev. B: Condens. Matter* **54**, 11169 (1994).
5. W. Kohn and L. J. Sham, *Phys. Rev.* **140**, 1133 (1965).
6. A. S. Fedorov, M. V. Serzhantova, and A. A. Kuzubov, *JETP* **107** (1), 126 (2008).
7. G. V. Vineyard, *J. Phys. Chem. Solids* **3**, 121 (1957).
8. G. Henkelman, B. P. Uberuaga, and H. Jónsson, *J. Chem. Phys.* **113**, 9901 (2000).
9. G. N. Churilov, I. V. Osipova, P. V. Novikov, V. A. Lopatin, A. S. Krylov, Ye. V. Tomashevich, and E. A. Petrakovskaya, *Fullerenes, Nanotubes, Carbon Nanostruct.* **18**, 584 (2010).

Translated by K. Shakhlevich